AIAA JOURNAL
Vol. 37, No. 2, February 1999

Three-Dimensional Temporal Instability of Compressible Gas Jets Injected in Liquids

Krishnan Subramaniam* and Ramkumar N. Parthasarathy†
University of Oklahoma, Norman, Oklahoma 73019
and
Kai-Ming Chiang‡
Ensure Company, Ltd., Tao-Yuan Hsien 326, Taiwan, Republic of China

A temporal linear stability analysis was conducted to study the growth rates of three-dimensional disturbances on a compressible inviscid gas jet injected into an incompressible viscous liquid coflow in the absence of gravitational effects. The primary parameters that governed the growth rates of the disturbances were the gas Weber number, Mach number, Ohnsorge number, density ratio, and velocity ratio. As the Mach number was increased, the range of unstable wave numbers and the growth rates of the unstable modes were increased. Also, the maximum growth rate was shifted to larger wave numbers (smaller wavelengths). The disturbance velocities were small, on the order of the coflowing liquid velocity. The growth rates and range of unstable wave numbers were reduced as the liquid coflow was increased. With an increase in liquid viscosity, the growth rates were reduced and the maximum growth rates were shifted to longer wavelengths. A reduction in the ratio of the liquid density to the mean gas density resulted in an increase in the growth rates of the unstable disturbances and the disturbance velocities.

Nomenclature

a = gas jet radius
c = speed of sound
I_n = nth-order modified Bessel function of the first kind
i = $\sqrt{-1}$
K_n = nth-order modified Bessel function of the second kind
k = wave number
Ma = Mach number
m = nondimensional wave number, ka
m_q = nondimensional q, qa
n = number representing the azimuthal mode
p = pressure
q = variable, $\sqrt{[k^2 + (\omega + ikU_g)^2/c^2]}$
r = radial distance
S_a = nondimensional s, sa
s = variable, $\sqrt{[k^2 + \rho_l(\omega + ikU_l)/\mu_l]}$
t = time
U = mean velocity of the fluid
u = disturbed velocity
We_g = gas Weber number, $\bar{\rho}_g U_g^2 a/\sigma$
Z = Ohnsorge number, $\mu_l/\sqrt{(\rho_l a\sigma)}$
z = axial distance
η = disturbance amplitude
θ = azimuthal angle
μ = dynamic viscosity
ρ = density ratio, $\rho_l/\bar{\rho}_g$
$\bar{\rho}_g$ = mean gas density
ρ_l = liquid density
σ = surface tension
τ = shear stress
Ω = nondimensional wave frequency, $\omega\sqrt{(\bar{\rho}_g a^3/\sigma)}$
ω = wave frequency

Subscripts

g = gas property
l = liquid property
lim = limiting value

I. Introduction

THE injection of gas jets into liquids is used in a number of practical applications, such as nuclear reactors, oxygenators, coal and mineral purifiers,[1] and the process of forming liquid shells.[2] The breakup of the gas jets and the resulting formation of gas bubbles play a vital role in these applications. In the past, a number of studies have focused on the breakup of liquid jets injected into gases; reviews are provided by Lefebvre,[3] Chigier and Reitz,[4] and Lin.[5] A few studies have been undertaken to investigate the stability characteristics of liquid layers adjacent to high-speed subsonic, supersonic, and sonic gas streams for cooling applications in atmospheric re-entry vehicles.[6–8] However, the instability characteristics of compressible gas jets injected into liquids have not been studied in detail.

Li and Bhunia[9] studied the temporal instability of plane incompressible gas sheets in a viscous liquid medium. Their results indicated that sinuous and varicose disturbances were unstable; surface tension reduced the growth rate, whereas the relative velocity between the gas and liquid and the gas density enhanced the growth rate of the disturbances. Also, the wave propagation velocity was much smaller than the gas velocity, implying that the disturbances were almost stationary and not the traveling-wave type. Radwan[10] considered the instability of a hollow incompressible gas jet with effects of surface tension and fluid inertia, neglecting the liquid viscosity; the gas inertia was found to have a destabilizing influence. Zhou and Lin[11,12] studied the absolute/convective instability of an inviscid, compressible liquid jet injected into a stationary, compressible, inviscid gas. It was assumed that the varicose mode was the fastest-growing disturbance. The growth rate and the range of unstable disturbances for the varicose mode were increased with an increase in the compressibility of the jet and ambient fluid; also, the compressibility of the ambient gas promoted absolute instability, as opposed to the compressibility of the liquid jet.

The objective of this investigation was to study the instability characteristics of a compressible gas jet injected into a coflowing viscous liquid medium, neglecting the effects of gravity. A linear temporal instability analysis, along the lines of Ref. 10, is used to document the wave growth rate as a function of wave number for a number of conditions. The details of the analysis are presented

Received May 4, 1998; revision received Aug. 13, 1998; accepted for publication Sept. 23, 1998.

*Graduate Student, School of Aerospace and Mechanical Engineering, 212 Felgar Hall, 865 Asp Avenue.
†Assistant Professor, School of Aerospace and Mechanical Engineering, 212 Felgar Hall, 865 Asp Avenue. Senior Member AIAA.
‡Deputy Engineer, Executive Office, 489, Hsin-Jung Road, Kao-Jung Li, Yung-Mei Town.

first, followed by a discussion of the results and a summary of conclusions.

II. Linear Stability Analysis

Consider a gas jet injected at uniform velocity U_g from a round nozzle of radius a into an infinite viscous incompressible liquid medium that is moving at a uniform velocity U_l; the force due to the pressure difference between the gas and liquid balances the surface tension force. A sharp velocity discontinuity is assumed at $r = a$. There is no heat or mass transfer between the liquid and gas. Gravitational effects are neglected. In addition, the gas is considered inviscid; the neglect of gas viscosity is based on the results from previous studies[13,14] of liquid sheet/jet breakup that effects of gas viscosity were small and did not significantly alter the instability characteristics.

A cylindrical coordinate system (z, r, θ) with the origin located at the nozzle exit and the positive z coordinate coincident with the jet centerline is used in the analysis. Small perturbations to the liquid and gas velocities, pressures, and gas density represented by $\boldsymbol{u}_l$, $\boldsymbol{u}_g$, p_l, p_g, and ρ_g are considered; the perturbed gas–liquid interface is represented by η. The linearized mass and momentum equations governing the disturbance velocities and pressures for the liquid are

$$\nabla \cdot \boldsymbol{u}_l = 0$$

$$\rho_l\left(\frac{\partial}{\partial t} + U_l\frac{\partial}{\partial z}\right)u_{lz} = \frac{-\partial p_l}{\partial z} + \mu_l\nabla^2 u_{lz}$$

$$\rho_l\left(\frac{\partial}{\partial t} + U_l\frac{\partial}{\partial z}\right)u_{lr} = \frac{-\partial p_l}{\partial r} + \mu_l\left(\nabla^2 u_{lr} - \frac{u_{lr}}{r^2} - \frac{2}{r^2}\frac{\partial u_{l\theta}}{\partial \theta}\right) \tag{1}$$

$$\rho_l\left(\frac{\partial}{\partial t} + U_l\frac{\partial}{\partial z}\right)u_{l\theta} = -\frac{1}{r}\frac{\partial p_l}{\partial \theta} + \mu_l\left(\nabla^2 u_{l\theta} - \frac{u_{l\theta}}{r^2} + \frac{2}{r^2}\frac{\partial u_{lr}}{\partial \theta}\right)$$

and for the gas are

$$\frac{\partial \rho_g}{\partial t} + U_g\frac{\partial \rho_g}{\partial z} + \bar{\rho}_g\left[\frac{\partial u_{gz}}{\partial z} + \frac{1}{r}\frac{\partial (r u_{gr})}{\partial r} + \frac{1}{r}\frac{\partial u_{g\theta}}{\partial \theta}\right] = 0 \tag{2}$$

$$\bar{\rho}_g\left(\frac{\partial}{\partial t} + U_g\frac{\partial}{\partial z}\right)\boldsymbol{u}_g = -\nabla p_g \tag{3}$$

The boundary conditions are linearized and applied at $r = a$. The kinematic boundary condition for the gas and liquid is

$$u_{l,gr} = \left(\frac{\partial}{\partial t} + U_{l,g}\frac{\partial}{\partial z}\right)\eta \tag{4}$$

The dynamic boundary conditions involve the balance of tangential and normal stresses. They are

$$\tau_{lr_z} = \mu_l\left(\frac{\partial u_{lr}}{\partial z} + \frac{\partial u_{lz}}{\partial r}\right) = 0 \tag{5}$$

$$\tau_{lr\theta} = \mu_l\left[r\frac{\partial}{\partial r}\left(\frac{u_{l\theta}}{r}\right) + \frac{1}{r}\frac{\partial u_{lr}}{\partial \theta}\right] = 0 \tag{6}$$

$$-p_l + 2\mu_l\frac{\partial u_{lr}}{\partial r} + p_g + \frac{\sigma}{a^2}\left(\eta + a^2\frac{\partial^2 \eta}{\partial z^2} + \frac{\partial^2 \eta}{\partial \theta^2}\right) = 0 \tag{7}$$

Also, symmetry conditions must be satisfied at $r = 0$; the disturbances must decay as $r \to \infty$.

We assume that the disturbances are in the form of normal modes

$$[\boldsymbol{u}_{l,g}; p_{l,g}; \eta] = [u_{lo,go}(r); p_{lo,go}(r); \eta_o]\exp[\omega t + i(kz + n\theta)] \tag{8}$$

The frequency ω is complex, with the real part ω_r denoting the growth rate of the disturbance and the imaginary part ω_i proportional to the disturbance frequency. The disturbances with $n = 0$ represent varicose waves, whereas those with $n = 1$ are sinuous waves. Elliptical cross sections are obtained for $n = 2$. For $n \geq 3$, deformations occur in both the axial and circumferential directions, and the disturbances grow on the jet surface.

The solutions of Eqs. (1) in the form given by Eq. (8) are

$$u_{lz} = [ikB_1K_n(kr) + B_2K_n(sr)]\exp[\omega t + i(kz + n\theta)]$$

$$u_{lr} = \left[kB_1K_n'(kr) + \frac{ik}{s}B_2K_{n-1}(sr) + B_3\frac{nK_n(sr)}{sr}\right]$$

$$\times \exp[\omega t + i(kz + n\theta)]$$

$$u_{l\theta} = i\left[\frac{n}{r}B_1K_n(kr) + \frac{ik}{s}B_2k_{n-1}(sr) + B_3K_n'(sr)\right] \tag{9}$$

$$\times \exp[\omega t + i(kz + n\theta)]$$

$$p_l = -\rho_l(\omega + ikU_l)B_1K_n(kr)\exp[\omega t + i(kz + n\theta)]$$

$$s^2 = k^2 + \frac{\rho_l}{\mu_l}(\omega + ikU_l)$$

where B_1, B_2, and B_3 are integration constants with appropriate dimensions and $K_n'(y) = \mathrm{d}K_n(y)/\mathrm{d}y$.

For the gas, the change in pressure can be related to the change in density as

$$\frac{\partial p_g}{\partial \rho_g} = c^2 \tag{10}$$

The dot product of the gradient operator with Eq. (3) gives

$$\bar{\rho}_g\left(\frac{\partial \nabla \cdot \boldsymbol{u}_g}{\partial t} + U_g\frac{\partial \nabla \cdot \boldsymbol{u}_g}{\partial z}\right) = -\nabla^2 p_g \tag{11}$$

which when combined with continuity equation (2) results in

$$\left(\frac{\partial^2 \rho_g}{\partial t^2} + 2U_g\frac{\partial^2 \rho_g}{\partial t\,\partial z} + U_g^2\frac{\partial^2 \rho_g}{\partial z^2}\right) = \nabla^2 p_g \tag{12}$$

Using Eq. (10), Eq. (12) is rewritten as

$$\frac{1}{c^2}\left(\frac{\partial^2 p_g}{\partial t^2} + 2U_g\frac{\partial^2 p_g}{\partial t\,\partial z} + U_g^2\frac{\partial^2 p_g}{\partial z^2}\right) = \nabla^2 p_g \tag{13}$$

The normal mode form of the solutions to Eqs. (2) and (13) is

$$p_g = -\bar{\rho}_g(\omega + ikU_g)AI_n(qr)\exp[\omega t + i(kz + n\theta)]$$

$$u_{gz} = ikAI_n(qr)\exp[\omega t + i(kz + n\theta)]$$

$$u_{gr} = qAI_n'(qr)\exp[\omega t + i(kz + n\theta)] \tag{14}$$

$$u_{g\theta} = \frac{in}{r}AI_n(qr)\exp[\omega t + i(kz + n\theta)]$$

$$q^2 = k^2 + \frac{(\omega + ikU_g)^2}{c^2}$$

where A is an integration constant with appropriate dimension and $I_n'(y) = \mathrm{d}I_n(y)/\mathrm{d}y$.

The constants A, B_1, B_2, and B_3 are evaluated using boundary conditions (4–6). The normal stress balance (7) then yields the following dispersion relation:

$$\rho\Omega_1^2\frac{\Delta_1}{\Delta} - \frac{1}{m_q}\frac{I_n(m_q)}{I_n'(m_q)}\Omega_2^2 + 2Z\rho^{\frac{1}{2}}\Omega_1\left\{m^2\frac{K_n''(m)}{K_n(m)}\frac{\Delta_1}{\Delta}\right.$$

$$+\frac{m^2}{S_a}\frac{K_{n-1}'(S_a)}{K_n'(S_a)}\Delta_2 + \left[\frac{S_aK_n'(S_a) - K_n(S_a)}{K_n(S_a)}\right]$$

$$\left.\times\left[1 - \frac{mK_n'(m)}{K_n(m)}\frac{\Delta_1}{\Delta} - \frac{m^2}{S_a^2}\frac{K_{n-1}(S_a)}{K_n'(S_a)}\Delta_2\right]\right\} + 1 - m^2 - n^2 = 0 \tag{15}$$

where

$$\Delta_1 = -n^2 + \frac{S_a F}{K_n(S_a)} - \frac{m^2}{S_a K_n'(S_a)}\left[nG + \frac{K_{n-1}(S_a)}{K_n(S_a)}F\right] \quad (16)$$

$$\Delta = -2n^2 + \frac{mK_n'(m)}{K_n(m)}\left[\frac{2S_a F}{K_n(S_a)} - \Delta_1\right] \quad (17)$$

$$\Delta_2 = 1 + \frac{mK_n'(m)}{K_n(m)}\frac{\Delta_1}{\Delta} \quad (18)$$

$$F = 2K_n'(S_a) - \left[S_a + \left(n^2/S_a\right)\right]K_n(S_a) \quad (19)$$

$$G = K_{n-1}'(S_a) - \frac{K_{n-1}(S_a)}{S_a} \quad (20)$$

$$\Omega_1 = \Omega + im(U_l/U_g)\sqrt{We_g} \quad (21)$$

$$S_a^2 = m^2 + \left(\rho^{\frac{1}{2}}/Z\right)\Omega_1 \quad (22)$$

$$\Omega_2 = \Omega + im\sqrt{We_g} \quad (23)$$

$$m_q^2 = m^2 + Ma^2\left[im + \left(\Omega/\sqrt{We_g}\right)\right]^2 \quad (24)$$

Note that for small Mach numbers $m_q \approx m$ and Eq. (15) reduces to the dispersion relation governing the growth of instabilities in incompressible gas jets injected into liquids, given by Parthasarathy and Chiang.[15] In particular, for the varicose mode ($n = 0$), Eq. (15) reduces to

$$\rho\Omega_1^2 + \frac{m}{m_q}\frac{I_0(m_q)}{I_1(m_q)}\frac{K_1(m)}{K_0(m)}\Omega_2^2 + 2Z\rho^{\frac{1}{2}}m^2\Omega_1\left[1 - \frac{K_1'(m)}{K_0(m)}\right] + 4Z^2m^3\left[\frac{S_aK_1'(S_a)}{K_1(S_a)}\frac{K_1(m)}{K_0(m)} - \frac{mK_1'(m)}{K_0(m)}\right] = \frac{mK_1(m)}{K_0(m)}(1 - m^2) \quad (25)$$

Before one solves the dispersion relations, it is of interest to compute the limiting wave number. An analysis of Eq. (25) indicates that the wave velocity is on the order of the coflowing liquid velocity in the absence of liquid viscous effects and is unaltered by gas compressibility effects.[16] The limiting wave number for the varicose mode is governed by the relation

$$m_{\lim q}\frac{m_{\lim}^2 - 1}{m_{\lim}^2}\frac{I_1\left(m_{\lim q}\right)}{I_0\left(m_{\lim q}\right)} = We_g\left(1 - \frac{U_l}{U_g}\right)^2 \quad (26)$$

where

$$m_{\lim q}^2 = m_{\lim}^2\left\{1 - Ma^2[1 - (U_l/U_g)]^2\right\} \quad (27)$$

For large gas injection velocities, corresponding to large We_g, the Bessel functions can be replaced by their asymptotic values, and we get

$$m_{\lim} \cong \frac{We_g[1 - (U_l/U_g)]^2}{\sqrt{1 - Ma^2[1 - (U_l/U_g)]^2}} \quad (28)$$

Thus, we see that the limiting wave number is increased from its value for the corresponding incompressible gas jet ($Ma = 0$), indicating that gas compressibility increases the range of unstable disturbances.

Equation (15) is solved using Muller's[17] method to document the wave growth rate as a function of wave number for given ρ, We_g, Z, Ma, and U_l/U_g. The solution is considered converged when the difference in the solution between successive iterations is less than 10^{-9}. Also, it was verified that the results corresponding to $Ma = 0$ were identical to those of Parthasarathy and Chiang.[15] At supersonic gas injection speeds, the presence of a shock wave at the injector exit must be considered, which is beyond the scope of the present study. Therefore we consider cases with $Ma < 1$ here.

III. Results

When the Mach number is small, the solutions of Eq. (15) correspond to the instability of an incompressible gas injected into a viscous liquid. Therefore, the case of $Ma = 0.1$ is considered first. The growth rates of various azimuthal modes, $n = 0$, 1, 2, and 3, are presented in Fig. 1 for the conditions $\rho = 1000$, $Z = 0.001$, and $U_l/U_g = 0$ for different gas Weber numbers (different gas injection velocities). These values of density ratio and Ohnsorge number are typical of air jets injected into water. It is observed that both the growth rates and the range of unstable wave numbers are increased with an increase in gas Weber number, highlighting the destabilizing role played by the gas injection velocity. The growth rate of the sinuous mode ($n = 1$) is slightly smaller than that of the varicose mode for small Weber numbers; the growth rate becomes comparable to that of the varicose mode as the Weber number is increased. The azimuthal mode corresponding to $n = 2$ has a much smaller growth rate than that of the varicose and sinuous modes at $We_g = 5$; however, the growth rate increases dramatically and becomes comparable to that of the varicose and sinuous modes at $We_g = 40$. A similar trend is observed in Fig. 1 for the $n = 3$ mode. This mode is stable at $We_g = 5$ and becomes unstable only for $We_g > 6$; the growth rate of this mode is the smallest of the growth rates of all of the modes at $We_g = 10$. For $We_g = 40$, the growth rate of this mode is only slightly smaller than the growth rate of the varicose and sinuous modes. It is also observed that, whereas the varicose and sinuous modes are unstable to very-long-wavelength disturbances (corresponding to $m = 0$), the modes $n = 2$ and 3 are unstable to disturbances of finite wavelengths only. A comparison of these results with those of Parthasarathy and Chiang[15] indicates that there is very little difference in the instability characteristics of the gas jet with $Ma = 0.1$ compared with an incompressible jet.

To highlight the effects of gas compressibility, the dispersion relation was solved for two values of Mach number: 0.5 and 0.8. The growth rates of the various azimuthal modes for $Ma = 0.8$ are presented in Fig. 2; the other conditions were kept identical to those of Fig. 1. It is seen that the maximum growth rate and the range of unstable wave numbers are increased with an increase in the Mach number for all of the Weber numbers considered. For example, at a gas Weber number of 10, the maximum growth rate of the varicose mode is increased from 0.46 to 0.8 when the Mach number is increased from 0.1 to 0.8. Similarly, for the $n = 3$ mode, the maximum growth rate doubles with an increase in Mach number from 0.1 to 0.8. The wave number corresponding to the maximum growth rate is also increased with increasing gas compressibility effects. For a gas Weber number of 10, the maximum growth rate of the varicose mode occurs at a wave number of 6.8 at $Ma = 0.1$, which is increased to 12 at $Ma = 0.8$. Similar observations are made for the other azimuthal modes over the range of Weber numbers considered. An increase in Mach number causes an increase in the gas pressure disturbance and the disturbance velocities that promote the growth of instabilities. Note that this is in contrast to the results of Zhou and Lin,[12] who found that increasing the compressibility of a liquid

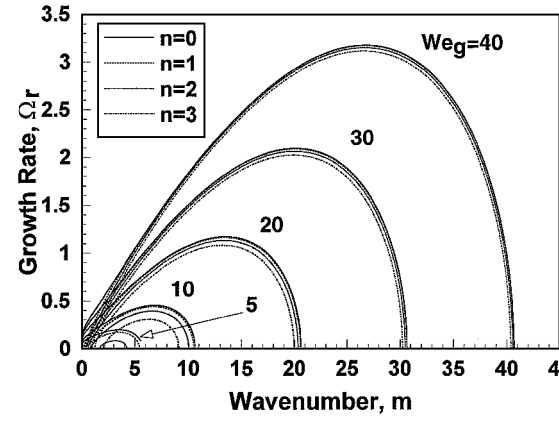

Fig. 1 Growth rates of the various azimuthal modes at different Weber numbers and small compressibility effects ($Ma = 0.1$, $\rho = 1000$, $Z = 0.001$, and $U_l/U_g = 0$).

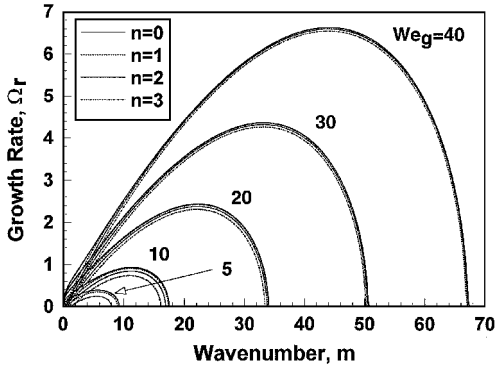

Fig. 2 Growth rates of the various azimuthal modes at different Weber numbers and significant compressibility effects ($Ma = 0.8$, $\rho = 1000$, $Z = 0.001$, and $U_l/U_g = 0$).

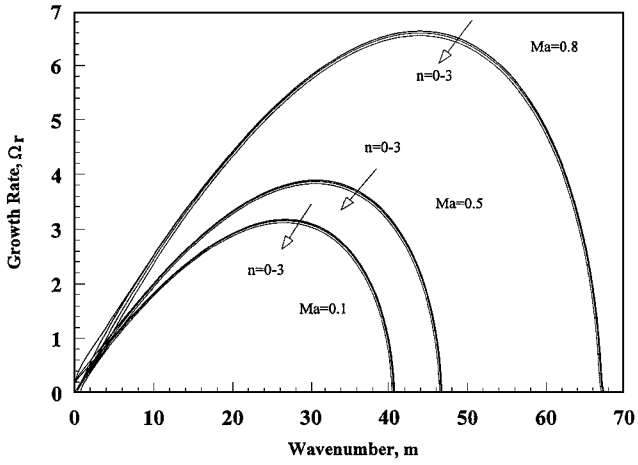

Fig. 3 Growth rates of the various azimuthal modes at different Mach numbers for fixed Weber number ($We_g = 40$, $\rho = 1000$, $Z = 0.001$, and $U_l/U_g = 0$).

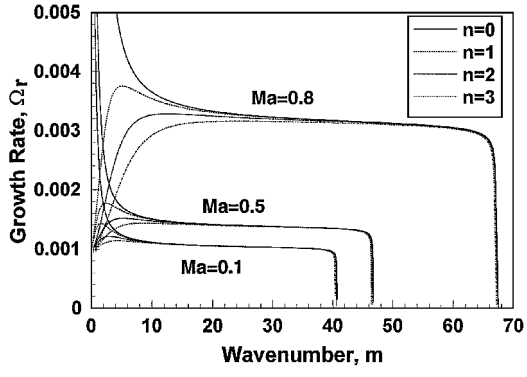

Fig. 4 Wave velocities of the various azimuthal modes at different Mach numbers ($We_g = 40$, $\rho = 1000$, $Z = 0.001$, and $U_l/U_g = 0$).

jet injected into a gas caused a reduction in the growth rate of the varicose mode; the range of unstable wave numbers was, however, increased.

A comparison of the growth rates of the various azimuthal modes for different Mach numbers is provided in Fig. 3 for $We_g = 40$, $\rho = 1000$, $Z = 0.001$, and $U_l/U_g = 0$. The effects of gas compressibility are clearly highlighted. Whereas there is no significant difference between the growth rates of the various azimuthal modes at the same Mach number, an increase in gas compressibility results in a significant increase in the growth rates of the instabilities and shifts the maximum growth rate to larger wave numbers (smaller wavelengths). The wave velocities of the various azimuthal modes under these conditions are displayed in Fig. 4. The normalized disturbance velocity for the varicose mode begins at 1 for disturbances of very

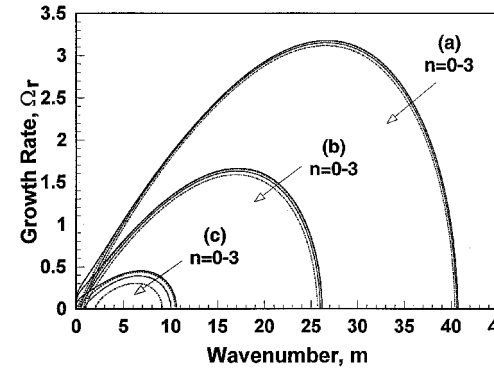

Fig. 5a Effect of velocity ratio on the growth rates at low Mach number ($Ma = 0.1$, $We_g = 40$, $\rho = 1000$, and $Z = 0.001$): a) $U_l/U_g = 0$, b) $U_l/U_g = 0.2$, and c) $U_l/U_g = 0.5$.

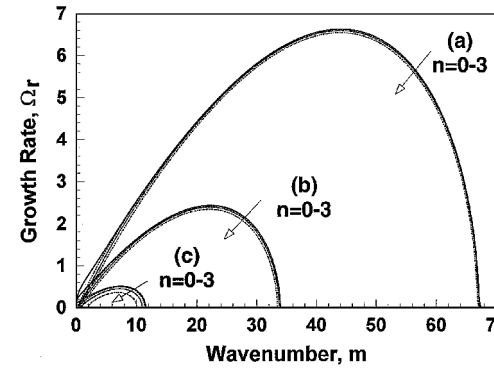

Fig. 5b Effect of velocity ratio on the growth rates with significant compressibility effects ($Ma = 0.8$, $We_g = 40$, $\rho = 1000$, and $Z = 0.001$): a) $U_l/U_g = 0$, b) $U_l/U_g = 0.2$, and c) $U_l/U_g = 0.5$.

long wavelengths and falls to a small value at finite wavelengths. An increase in the Mach number results in an increase in the disturbance velocity. The wave velocities of the $n = 1, 2, 3$ azimuthal modes remain small throughout the range of unstable wavelengths. It can be shown that the wave velocities are close to the coflowing liquid velocity.[16] Thus, these disturbances will appear stationary in a coordinate system moving with the liquid. Similar observations were made by Li and Bhunia[9] in the analysis of temporal instability of gas sheets injected into stationary liquids; it was found that the wave velocity was small compared with the injected gas velocity.

The effects of the coflowing liquid velocity on the instability characteristics are highlighted in Figs. 5a and 5b. The growth rates are plotted for $We_g = 40$, $\rho = 1000$, $Z = 0.001$, and $U_l/U_g = 0$, 0.2, and 0.5, with $Ma = 0.1$ (Fig. 5a) and 0.8 (Fig. 5b). Both the growth rates and the range of unstable wave numbers are reduced with an increase in the liquid coflow velocity. Also, the maximum growth rate is shifted to smaller wave numbers (or longer wavelengths). An increase in the liquid velocity results in a lower relative velocity, leading to a reduction in the destabilization. A comparison of the results for $Ma = 0.8$ with those for $Ma = 0.1$ indicates two interesting results. First, the difference in the growth rates between the various azimuthal modes $n = 0$, 1, 2, and 3 is reduced at the higher Mach number for all liquid coflow velocities. Thus, the compressibility of the gas jet leads to the instability of the jet to three-dimensional disturbances for all of the liquid coflow conditions considered here. Second, the effects of compressibility are significantly higher for small coflow velocities. Going from $Ma = 0.1$ to 0.8, the increase in the maximum growth rate is marginal for $U_l/U_g = 0.2$ and 0.5, whereas it becomes dramatic (more than doubled) for $U_l/U_g = 0$. Thus, under conditions when a significant liquid coflow is present, an increase in the compressibility of the gas jet does not significantly improve its instability characteristics.

The influence of liquid viscosity on the growth rates of the unstable disturbances is seen in Figs. 6a and 6b. Here the growth rates are

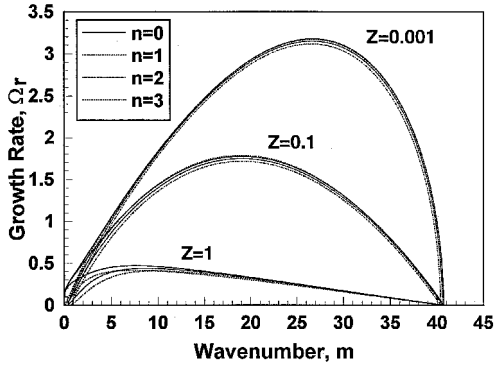

Fig. 6a Variation of growth rates with Ohnsorge number at low Mach number ($Ma = 0.1$, $We_g = 40$, $\rho = 1000$, and $U_l/U_g = 0$).

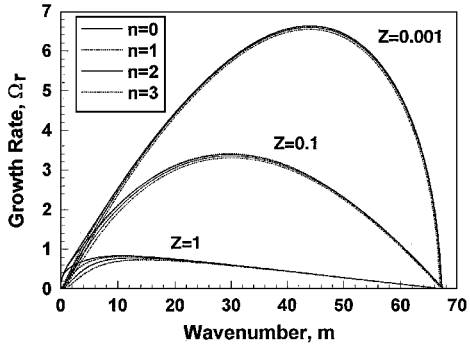

Fig. 6b Variation of growth rates with Ohnsorge number at conditions with significant compressible effects ($Ma = 0.8$, $We_g = 40$, $\rho = 1000$, and $U_l/U_g = 0$).

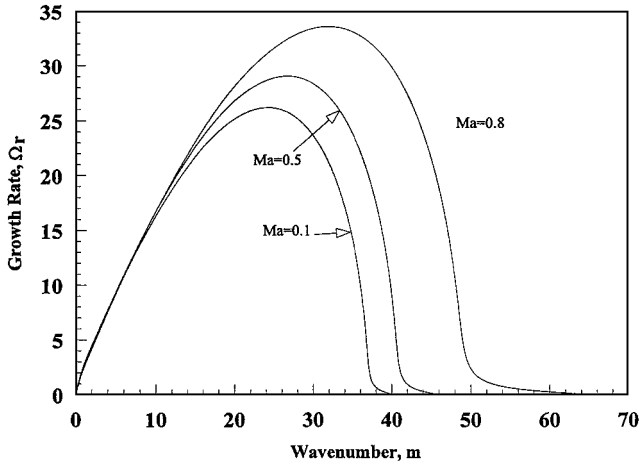

Fig. 7 Growth rates of the varicose mode at different Mach numbers and low density ratio ($We_g = 40$, $\rho = 10$, $Z = 0.001$, and $U_l/U_g = 0$).

plotted for $We_g = 40, \rho = 1000, U_l/U_g = 0$, and $Z = 0.001, 0.1$, and 1, with $Ma = 0.1$ (Fig. 6a) and 0.8 (Fig. 6b). An increase in liquid viscosity results in a decrease in the growth rates and the shifting of the maximum growth rates to smaller wave numbers (longer wavelengths). The range of unstable wave numbers remains unaltered. This is because an increase in the liquid viscosity causes an increase in the liquid normal stress [Eq. (7)] that resists the growth of the disturbance, thus promoting the stability of the gas jet. We see that the changes resulting from the increase in liquid viscosity are comparable at $Ma = 0.1$ and 0.8. Note that at $Ma = 0.1$ and $Z = 0.1$ the sinuous disturbance has a slightly higher growth rate than the varicose disturbance. Thus, depending on the liquid viscosity, the sinuous disturbance rather than the varicose disturbance may be the fastest-growing disturbance. However, at $Ma = 0.8$, the varicose disturbance remains the fastest-growing disturbance at all values of Z under these conditions.

Finally, the influence of the density ratio is illustrated in Fig. 7. The growth rates of the varicose mode are presented for $We_g = 40$, $Z = 0.001$, $U_l/U_g = 0$, and $\rho = 10$, 100, and 1000. A decrease in the density ratio is equivalent to a decrease in the liquid density and, therefore, the liquid pressure disturbance, which promotes the growth of disturbances. Thus, as the density ratio is decreased, the growth rates are increased (comparing Fig. 7 with Fig. 3); however, the range of unstable wave numbers remains unaltered. The wave number corresponding to the maximum growth rate is now shifted to lower values, indicating that the maximum growth rate occurs at longer wavelengths with a decrease in the density ratio. It is also observed that the effects of gas compressibility are not significant at a small density ratio; the maximum growth rate and the wave number corresponding to the maximum growth rate are increased only by 35 and 50%, respectively, as the Mach number is increased from 0.1 to 0.8 at $\rho = 10$.

IV. Conclusions

In summary, a temporal linear stability analysis was conducted to study the growth rates of three-dimensional disturbances on a compressible inviscid gas jet injected into an incompressible viscous liquid coflow in the absence of gravitational effects. The primary parameters that governed the growth rates of the disturbances were the gas Weber number, Mach number, Ohnsorge number, density ratio, and velocity ratio. For small Mach numbers, only the varicose mode was unstable at low Weber numbers; as the gas Weber number was increased, higher-order azimuthal modes became unstable, with growth rates comparable to those of the varicose mode. As the Mach number was increased, the range of unstable wave numbers and the growth rates of the unstable modes were increased. Also, the maximum growth rate was shifted to larger wave numbers. Thus, the breakup of gas jets injected into liquids can be significantly aided by injecting at speeds when compressibility effects are important. At these high injection speeds, the higher-order azimuthal modes become unstable, causing the jet breakup to occur on the surface rather than as a whole jet.

The disturbance velocities were small, on the order of the coflowing liquid velocity. Thus, the disturbances on the gas jet would appear stationary in a coordinate system moving with the liquid. An increase in the liquid coflow velocity caused a decrease in the range of unstable wave numbers and the growth rates and a shifting of the maximum growth rate to smaller wave numbers. The liquid viscosity played a significant role in the growth of instabilities. The growth rates were reduced, and the maximum growth rate was shifted to smaller wave numbers as the liquid viscosity was increased. The range of unstable wave numbers, however, remained unchanged. Depending on the liquid viscosity, under certain conditions, the sinuous disturbance might be the fastest-growing disturbance. The ratio of liquid density to mean gas density was another important variable. A reduction in the liquid density greatly increased the growth rates of the unstable disturbances while maintaining the same range of unstable wave numbers. Unfortunately, only limited experimental measurements exist on the breakup of gas jets injected into liquids. The authors are not aware of any experiments with compressible gas jets with which to compare the present results.

Acknowledgments

The authors are grateful to the reviewers for their comments and valuable input to the paper.

References

[1] Leonard, J. W., III, *Coal Preparation*, 5th ed., Society of Mining, Metallurgy, and Exploration, Littleton, CO, 1991, Chap. 3.

[2] Kendall, J. M., "Experiments on Annular Liquid Jet Instability and on the Formation of Liquid Shells," *Physics of Fluids*, Vol. 29, No. 7, 1986, pp. 2086–2094.

[3] Lefebvre, A. H., *Atomization and Sprays*, Hemisphere, New York, 1989, Chap. 2.

[4] Chigier, N., and Reitz, R. D., "Regimes of Jet Breakup and Breakup Mechanisms (Physical Aspects)," *Recent Advances in Spray Combustion: Spray Atomization and Drop Burning Phenomena*, edited by K. K. Kuo, Vol. 166, Progress in Astronautics and Aeronautics, AIAA, Reston, VA, 1996, pp. 109–135.

[5]Lin, S. P., "Regimes of Jet Breakup and Breakup Mechanisms (Mathematical Aspects)," *Recent Advances in Spray Combustion: Spray Atomization and Drop Burning Phenomena*, edited by K. K. Kuo, Vol. 166, Progress in Astronautics and Aeronautics, AIAA, Reston, VA, 1996, pp. 137–160.

[6]Chang, I. D., and Russell, P. E., "Stability of a Liquid Layer Adjacent to a High Speed Gas Stream," *Physics of Fluids*, Vol. 8, No. 6, 1965, pp. 1018–1026.

[7]Chawla, T. C., "The Kelvin–Helmholtz Instability of the Gas–Liquid Interface of a Sonic Gas Jet Submerged in a Liquid," *Journal of Fluid Mechanics*, Vol. 67, 1975, pp. 513–537.

[8]Nayfeh, A. H., and Saric, W. S., "Nonlinear Stability of Liquid Film Adjacent to a Supersonic Stream," *Journal of Fluid Mechanics*, Vol. 58, 1973, pp. 209–231.

[9]Li, X., and Bhunia, A., "Temporal Instability of Plane Gas Sheets in a Viscous Liquid Medium," *Physics of Fluids*, Vol. 8, No. 1, 1996, pp. 103–111.

[10]Radwan, A. E., "Instability of a Hollow Jet with Effects of Surface Tension and Fluid Inertia," *Journal of the Physical Society of Japan*, Vol. 58, No. 4, 1989, pp. 1225–1227.

[11]Zhou, Z. W., and Lin, S. P., "Absolute and Convective Instability of a Compressible Jet," *Physics of Fluids A*, Vol. 4, No. 2, 1992, pp. 277–282.

[12]Zhou, Z. W., and Lin, S. P., "Effects of Compressibility on the Atomization of Liquid Jets," *Journal of Propulsion and Power*, Vol. 8, No. 4, 1992, pp. 736–740.

[13]Lin, S. P., and Lian, Z. W., "Mechanisms of the Breakup of Liquid Jets," *AIAA Journal*, Vol. 28, No. 1, 1990, pp. 120–126.

[14]Witherspoon, W., and Parthasarathy, R. N., "Breakup of Viscous Liquid Sheets Subjected to Symmetric and Asymmetric Gas Flow," *Journal of Energy Resources Technology*, Vol. 119, No. 3, 1997, pp. 184–192.

[15]Parthasarathy, R. N., and Chiang, K.-M., "Temporal Instability of Gas Jets Injected in Viscous Liquids to Three-Dimensional Disturbances," *Physics of Fluids*, Vol. 10, No. 8, 1998, pp. 2105–2107.

[16]Chiang, K.-M., "Temporal Instability of Inviscid Gas Jets Injected in Liquids," M.S. Thesis, School of Aerospace and Mechanical Engineering, Univ. of Oklahoma, Norman, OK, Dec. 1996.

[17]Muller, D. E., "A Method for Solving Algebraic Equations Using an Automatic Computer," *Mathematical Tables and Other Aid to Computation*, Vol. 10, No. 5, 1956, pp. 208–212.

J. P. Gore
Associate Editor